Spin splitting in pseudomorphic $In_xGa_{1-x}As/In_yAl_{1-y}As$ graded heterostructures

Y. S. Gui, C. M. Hu, Z. H. Chen, G. Z. Zheng, S. L. Guo, and J. H. Chu
National Laboratory for Infrared Physics, Shanghai Institute of Technical Physics, Chinese Academy of Sciences, Shanghai 200083, China

J. X. Chen and A. Z. Li
National Laboratory of Functional Materials for Informatics, Shanghai Institute of Metallurgy, Chinese Academy of Sciences, Shanghai 200050, China

(Received 3 June 1999)

We have measured the spin splitting in the whole magnetic-field range in an $In_{0.80}Ga_{0.20}As/In_{0.53}Ga_{0.47}As/In_{0.52}Al_{0.48}As$ graded heterostructure, and found that the spin splitting did not go to zero at any magnetic field, in agreement with recent theoretical predictions. A zero-field spin splitting of 3.82 ± 0.09 meV and an effective g factor as a function of magnetic field are deduced.

Zero-field and non-zero-field spin splitting of electric subbands in III-V semiconductor heterostructures have attracted considerable and continuously growing theoretical and experimental interest.[1–7] In a semiconductor heterostructure, the spin splitting of the subband states at $B=0$ is ascribed to bulk inversion asymmetry (BIA),[8–12] which dominants in wide-gap materials such as $GaAs/Al_xGa_{1-x}As$, and to structure inversion asymmetry (SIA), which becomes important in narrow-gap systems such as InAs/GaSb, $In_xGa_{1-x}As/In_xAl_{1-x}As$ and $In_xGa_{1-x}As/InP$.[13–17] Recently, Pfeffer and co-workers[18–20] found that both BIA and SIA were of importance even in $GaAs/Al_xGa_{1-x}As$ heterostructures. For an increasing magnetic field, both BIA and SIA terms become less important, and total splitting is dominated by the non-zero-field spin splitting (Zeeman splitting), which is caused by an applied external magnetic field. The authors of Ref. 8 calculated the effect of an external magnetic field B on the spin splitting in $GaAs/Al_xGa_{1-x}As$ heterostructures, taking into account only the BIA mechanism, and concluded that the spin-splitting changes sign as a function of the external magnetic field B. Pfeffer and co-workers,[18–20] considering both BIA and SIA mechanisms, showed that the spin splitting does not change sign. Unfortunately, up to now no clear experimental data of the spin splitting as a function of magnetic field are available.

In this paper we study the magnetic-field-dependent spin splitting in a modulation-doped pseudomorphic $In_{0.80}Ga_{0.20}As/In_{0.53}Ga_{0.47}As/In_{0.52}Al_{0.48}As$ graded heterostructure with a high electron density ($n_s\sim2.5\times10^{12}\,cm^{-2}$) in the whole B range. Up to seven nodes in the beating pattern in the Shubnikov–de Haas (SdH) oscillations for a magnetic field in the range $0.20\,T<B<1.7\,T$ have been observed. The zero-field spin splitting and effective g factor were derived by fitting the B-dependent spin splitting.

The sample used in this work was grown on an Fe-doped semi-insulating InP substrate by molecular-beam epitaxy with a gas source. The structure consists of a 50-nm undoped $In_{0.52}Al_{0.48}As$ buffer, followed by a 20-nm undoped $In_{0.53}Ga_{0.47}As$ layer, a 6-nm undoped $In_{0.80}Ga_{0.20}As$ channel, a 6-nm undoped $In_{0.52}Al_{0.48}As$ layer, a silicon δ-doped ($5\times10^{12}\,cm^{-2}$) $In_{0.52}Al_{0.48}As$ layer, a 20-nm undoped $In_{0.40}Al_{0.60}As$ layer, and finally a 13-nm Si-doped ($3\times10^{18}\,cm^{-3}$) $In_{0.53}Ga_{0.47}As$ layer for Ohmic contacts. Magnetotransport measurements were performed in the Van der Pauw configuration with indium contacts at four sample corners. The experimental setups for obtaining the Hall resistance and SdH oscillations consisted of two separate systems: a ^{3}He cryostat ($T=0.3$ K) and a superconducting coil capable of magnetic fields up to 7 T, and a ^{4}He cryostat ($T=1.2$ K) and superconducting coil capable of magnetic fields up to 12 T. The Hall mobility and sheet electron density are $7.5\times10^4\,cm^2/V\,s$ and $2.56\times10^{12}\,cm^{-2}$ at 4.2 K, respectively.

The resistivity ρ_{xx} and ρ_{xy} measured at 0.3 K are shown in Fig. 1 as a function of the magnetic field (B) perpendicular to the two-dimensional (2D) layer. We can clearly observe SdH oscillations and quantum Hall plateaus at high magnetic field, as well as a pronounced beating effect at low magnetic field. A careful studying of the beat pattern was made by a very slowly B-changed measurement, and the second derivation plot of ρ_{xx} obtained by nine-point smoothing is shown in Fig 1(b), where the node positions do not shift that compared with the original curve of ρ_{xx} vs B. Seven distinct nodes in the beat pattern can be observed in the traces. The last node occurs at a magnetic field of 1.626 T. The beat in SdH oscillation arise from two sets of oscillations with slightly different frequencies caused by the presence of two kinds of carriers in the system. Fast Fourier transform (FFT) of ρ_{xx} as a function of $1/B$ is taken with a magnetic-field range between 0.247 and 0.844 T (see Fig. 2). The beat pattern in ρ_{xx} leads to a double-peak structure in the FFT spectrum. If we assume that two subbands are occupied, the sum of the electron concentration taken from the double-peak structure is exactly twice as high as the Hall concentration, indicating that we have to deal with a single 2D subband split into two non-spin-degenerate subbands. We therefore determine the concentrations $n_\pm$ corresponded to the two spin levels to be 1.23×10^{12} and $1.27\times10^{12}\,cm^{-2}$, respectively.

The obtained spin-resolved concentrations allow us to determine the spin-orbit interaction parameter α, which is an important coefficient. It is still an open question whether α is simply proportional to the average electric field $\langle E\rangle$ in the 2D

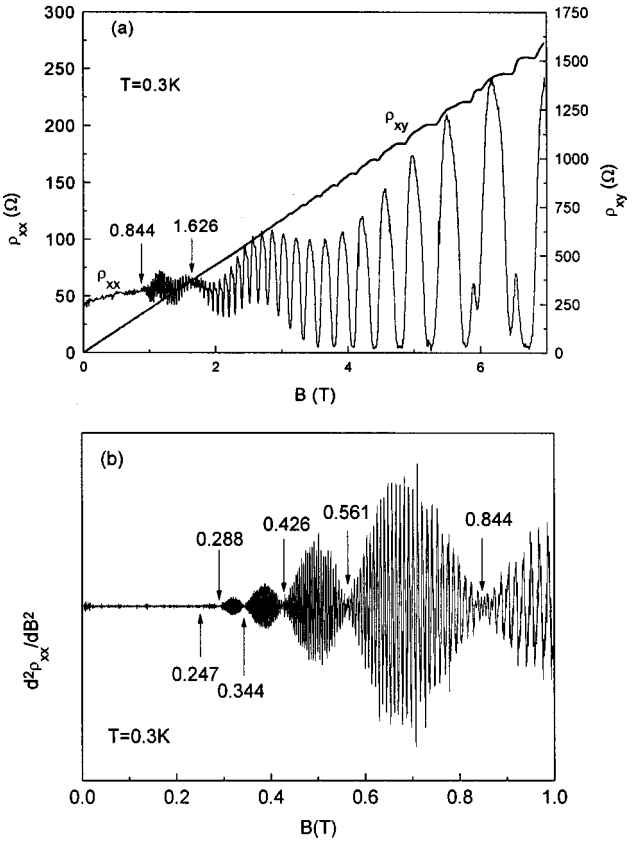

FIG. 1. (a) Resistivity ρ_{xx} and ρ_{xy} for sample A as a function of magnetic field at $T=0.3$ K. (b) The second derivative of ρ_{xx} for sample A as a function of magnetic field at $T=0.3$ K. Node positions in the SdH oscillation are marked by arrows.

channel.[8,16,20] By taking the average value $n=n_-+n_+$ and the difference $\Delta n=n_+-n_-$ of the electron concentrations, we determine the spin-orbit interaction parameter of our structure by using the following expression:[16,17]

$$\alpha=\frac{\Delta n\hbar^2}{m^*}\left(\frac{\pi}{2(n-\Delta n)}\right)^{1/2}. \tag{1}$$

The obtained α value of 0.525×10^{-11} eV m is of the same order as the previously obtained values of 0.9×10^{-11} eV m

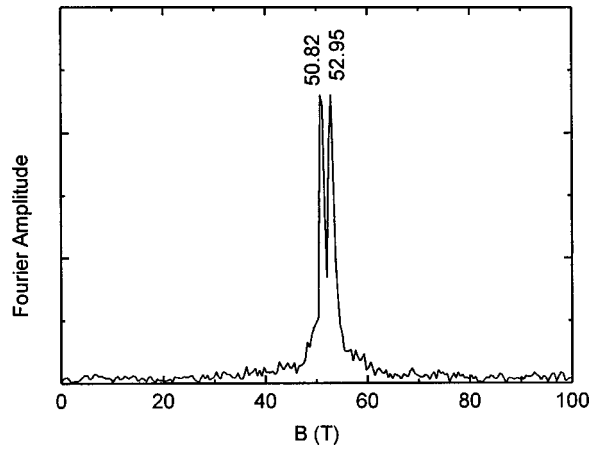

FIG. 2. Fast Fourier transform of the SdH oscillation taken with a magnetic-field range from 0.247 to 0.844 T at $T=0.3$ K.

in an InAs/GaSb quantum well,[14,15] $0.4-0.95\times10^{-11}$ eV m in an $In_xGa_{1-x}As/In_xAl_{1-x}As$ system,[4,13] $0.63-1.53\times10^{-11}$ eV m in an $In_xGa_{1-x}As/InP$ quantum[17,18] and 0.6×10^{-11} eV m in an InAs/AlSb quantum well.[5,6]

The low-field spin splitting can be extracted from the nodes in the beat pattern in the SdH oscillation. The numbers of rapid oscillations between the adjacent nodes are found to be 24, 26, 27, 29, 31, and 33 with increasing B. Since the spin splitting energy Δ is inversely proportional to the number of oscillation between two nodes, our data indicate that Δ decreases with increasing B for $B<1.626$ T. As discussed in Ref. 3 the spin splitting leads to a modulation of the SdH amplitude,

$$A\sim\cos\pi v, \tag{2}$$

where $v=\Delta/\hbar\omega_c$. Nodes in the beating pattern will occur at a half-integer value of v (±0.5, ±1.5, etc.). By assuming that the last node ($B=1.626$ T) corresponds to $v=0.5$, and the successively lower nodes occur at $v=1.5$, 2.5, etc., we determine the low-field spin splitting energies based on the nodes position indicated in Fig. 1.

For high magnetic fields where $\sigma_{xy}\gg\sigma_{xx}$, the transverse resistivity ρ_{xx} is given as

$$\rho_{xx}=\frac{\sigma_{xx}}{\sigma_{xx}^2+\sigma_{xy}^2}\approx\frac{\sigma_{xx}}{\sigma_{xy}^2}=\sigma_{xx}(h/e^2i)^2, \tag{3}$$

and the magnetoconductance of a two-dimensional electron gas at $T=0$ K is given by

$$\sigma_{xx}\propto\sum_{n^\pm}(n\pm1/2)\exp\left(-\frac{(E_F-E_n^\pm)^2}{\Gamma^2}\right), \tag{4}$$

where E_F is Fermi energy, Γ is the Landau-level broadening, and $E_n^\pm$ is the energy of the nth Landau level with spin-up $(+)$ and spin-down $(-)$.

These equations clearly show a maximum in ρ_{xx} each time a Landau level passes through the Fermi energy, and a minimum when the Fermi energy is situated between two Landau levels. By comparing the filling factor i derived from the step structures in the ρ_{xy} curve, we confirmed that spin splitting is directly observed in the curve ρ_{xx} $B>1.7$ T. As an approximation, the spin-splitting energy can be obtained by the equation[21]

$$\Delta\left(\frac{B_{n+}+B_{n-}}{2}\right)=\left(n+\frac{1}{2}\right)\frac{(B_{n-}-B_{n+})e\hbar}{m^*}, \tag{5}$$

where B_{n+} and B_{n-} are experimental values of the magnetic field when spin-up and -down levels of the nth Landau level pass through the Fermi level, respectively.

Figure 3 summaries the magnetic-field-dependent spin-splitting energies derived by nodes in a beating pattern at low field (open squares), and spin-resolved Landau levels at high field (solid squares). According to the calculations of Pfeffer and co-workers,[18–20] the spin splitting dominated by BIA and SIA mechanisms is predicted to decrease first as the magnetic field increases from zero, and only to increase with magnetic field when the Zeeman term is larger than the in-

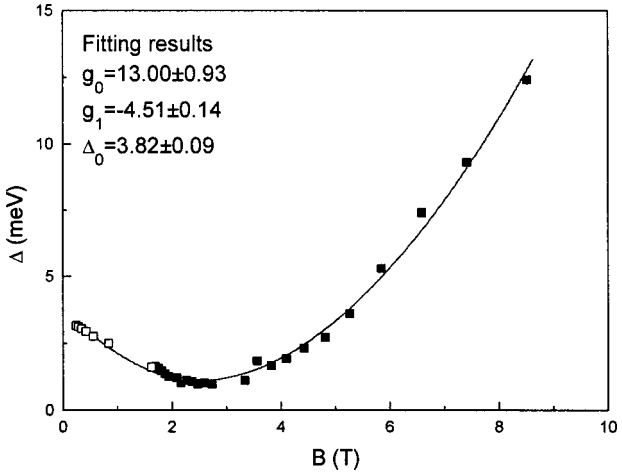

FIG. 3. Total spin splitting for sample *A* as a function of magnetic field. The open and solid squares are the experimental data derived by the nodes in beating pattern at low field and spin-resolved Landau levels at high field, respectively. The solid line is the theoretical fit. All data were derived from the experimental results at 0.3 K except for the last two data measured at 1.2 K.

version asymmetry term. It is also predicted that the spin splitting does not change sign in the whole magnetic field range. Our measured spin splitting that does not go to zero at any magnetic field agrees well with this calculation.

It is well known that zero-field spin splitting and Zeeman spin splitting are the dominant mechanisms in the low- and high-field ranges, respectively. In our measurement configuration B is applied along the z direction, so spin-up and -down related to the Zeeman term also refer to the z direction. The zero-field spin splitting is caused by spin-orbit interaction. The moving carriers in a quantum well ''feel'' an effective magnetic field, proportional to the vector product of the carriers' in-plane velocity and an electric field **E** perpendicular to the plane caused by the inversion asymmetry. Therefore spin-orbit interaction is related to an in-plane effective magnetic field. If BIA is neglected, one can obtain the spin-splitting energies for the SIA mechanism analytically. For high Landau numbers n, one obtains a good approximation[13]

$$\Delta(B)=[(\hbar\omega_c-g^*\mu_B B)^2+\Delta_0^2]^{1/2}-\hbar\omega_c, \qquad (6)$$

where Δ_0 is the zero-B spin-splitting energy, and $g^*=g_0+g_1B$ is the effective g factor which is significant nonlinear for $In_xGa_{1-x}As$.

We have used Eq. (6) to fit the experimental data with Δ_0, g_0, and g_1 as the fitting parameters. A very good agreement is found with all experimental data using $\Delta_0=3.82\pm0.09$ meV, $g_0=13.00\pm0.93$, and $g_1=-4.51\pm0.14$. The zero-B spin-splitting energy Δ_0 is slightly difference from the value of 2.5–2.75 meV reported in Ref. 13, and that of 4.5–5.9 meV from Ref. 4, and the difference can be attributed to the variation in the alloy composition and the carrier concentration. The effective g factor is significantly enhanced compared with its bandage value of ~2.3 in our sample; however, it lies in the range between 5 and 15 for $In_xGa_{1-x}As/In_xAl_{1-x}As$ and between 3 and 13 for the $In_xGa_{1-x}As/InP$ heterostructure reported by other authors.[22–24]

In conclusion, we have measured the spin-splitting energy of subband Landau levels in an $In_xGa_{1-x}As/In_xAl_{1-x}As$ graded heterostructure at Fermi energy. We obtained the spin-splitting energy as a function of external magnetic field in the whole B range, and found that spin splitting did not vanish at a finite magnetic field. A zero-field splitting with a value of $\Delta_0=3.82\pm0.09$ meV and a magnetic-field-dependent effective g factor with $g_0=13.00\pm0.93$, and $g_1=-4.51\pm0.14$ were determined.

The authors would like to acknowledge financial support from the Chinese Academy of Sciences and the National Natural Science Foundation of China.

[1] S. J. Papadaki, E. P. De Poortere, H. C. Manoharan, M. Shayegan, and R. Winkler, Science **283**, 2056 (1999).
[2] S. Datta and B. Das, Appl. Phys. Lett. **56**, 665 (1990).
[3] B. Das, D. C. Miller, S. Datta, R. Reifenberger, W. P. Hong, P. K. Bhattacharya, J. Sing, and M. Jaffe, Phys. Rev. B **38**, 1411 (1989).
[4] J. Nitta, T. Akazaki, and H. Takayanagi, Phys. Rev. Lett. **78**, 1335 (1997).
[5] J. P. Heida, B. J. van Wees, T. M. Klapwijk, and G. Borghs, in *Proceedings of the 23rd International Conference on the Physics of Semiconductors*, edited by M. Scheffler and R. Zimmermann (World Scientific, Singapore, 1996), Vol. 3, p. 2467.
[6] J. P. Heida, B. J. van Wees, J. J. Kuipers, T. M. Klapwijk, and G. Borghs, Phys. Rev. B **57**, 11 911 (1998).
[7] J. P. Lu, J. B. Yau, S. P. Shukla, M. Shayegan, L. Wissinger, U. Rossler, and R. Winkler, Phys. Rev. Lett. **81**, 1282 (1998).
[8] G. Lommer, F. Malcher, and U. Rossler, Phys. Rev. Lett. **60**, 728 (1988).
[9] R. Eppenga and M. F. H. Schuurmans, Phys. Rev. B **37**, 10 923 (1988).
[10] H. Riechert, S. Alvarado, A. N. Tikov, and I. Safarov, Phys. Rev. Lett. **52**, 2297 (1984).
[11] N. E. Christensen and M. Cardona, Solid State Commun. **51**, 491 (1984).
[12] P. D. Dresselhaus, C. M. A. Papavassiliou, R. G. Wheeler, and R. N. Sacks, Phys. Rev. Lett. **68**, 106 (1992).
[13] B. Das, S. Datta, and R. Reifenberger, Phys. Rev. B **41**, 8278 (1990).
[14] J. Luo, H. Munekata, F. F. Fang, and P. J. Stiles, Phys. Rev. B **38**, 10 142 (1988).
[15] J. Luo, H. Munekata, F. F. Fang, and P. J. Stiles, Phys. Rev. B **41**, 7685 (1990).
[16] G. Engels, J. Lange, Th. Schapers, and H. Luth, Phys. Rev. B **55**, R1958 (1997).
[17] Th. Schapers, G. Engels, J. Lange, Th. Klocke, M. Hollfelder, and H. Luth, J. Appl. Phys. **83**, 4324 (1998).
[18] P. Pfeffer and W. Zawadzki, Phys. Rev. B **52**, R14 332 (1995).
[19] P. Pfeffer, Phys. Rev. B **55**, R7359 (1997).
[20] P. Pfeffer and W. Zawadzki, Phys. Rev. B **59**, R5312 (1999).
[21] J. G. Savel'ev, A. M. Kreshchuk, S. V. Novikov, A. Y. Shik, G.

Remeny, G. Kovacs, B. Podor, and G. Gombos, J. Phys.: Condens. Matter **8**, 9025 (1996).
[22] J. C. Portal, R. J. Nicholas, M. A. Brummel, A. Y. Cho, K. Y. Cheng, and T. P. Pearsall, Solid State Commun. **43**, 907 (1982).
[23] R. J. Nicholas, M. A. Brummel, J. C. Portal, M. Razeghi, and M. A. Poisson, Solid State Commun. **43**, 825 (1982).
[24] D. L. Vehse, S. G. Hummell, H. M. Cox, F. de Rosa, and S. J. Allen, Phys. Rev. B **33**, 5862 (1986).